

## INTERNAL PRESSURE DISTRIBUTION CHARACTERISTICS OF INDUSTRIAL GLOBE VALVES

Fu-Yi Zhang<sup>1</sup>, Zhou-Yuan Cao<sup>1</sup>, Ji-Wei Shen<sup>1</sup>, Zhen-Jie Liu\*<sup>2</sup>

<sup>1</sup>College of Mechanical Engineering, Quzhou University, Quzhou, 324000, China.

<sup>2</sup>Quzhou Special Equipment Inspection & Testing Research Institute, Quzhou 324000, China.

Article Received on 21/02/2026

Article Revised on 14/03/2026

Article Published on 01/04/2026

### \*Corresponding Author

**Zhen-Jie Liu**

Quzhou Special Equipment  
Inspection & Testing Research  
Institute, Quzhou 324000, China.

<https://doi.org/10.5281/zenodo.19343432>



**How to cite this Article:** Fu-Yi Zhang<sup>1</sup>, Zhou-Yuan Cao<sup>1</sup>, Ji-Wei Shen\*<sup>1</sup>, Zhen-Jie Liu<sup>2</sup>. (2026). Internal Pressure Distribution Characteristics of Industrial Globe Valves. World Journal of Engineering Research and Technology, 12(4), 73–83.

This work is licensed under Creative Commons Attribution 4.0 International license.

### ABSTRACT

To investigate the internal pressure distribution patterns of industrial globe valves under varying operating conditions, thereby enhancing valve operational stability and system efficiency, this study employs SolidWorks to establish a three-dimensional geometric model of an industrial globe valve. Computational meshing is performed using ICEM, followed by numerical simulation. Results indicate: Under half conditions, a distinct high-pressure concentration zone exists at the valve orifice, with a tendency for low-pressure vortex zones to form downstream, posing cavitation risks; - Under fully open conditions, pressure distribution becomes more uniform, local resistance is significantly reduced, and system efficiency is enhanced. These findings provide theoretical support for structural optimisation,

operating condition selection, and safe operation of industrial globe valves.

**KEYWORDS:** Globe valve, numerical calculation, pressure distribution, localised resistance.

### 1. INTRODUCTION

Industrial globe valves, serving as critical control components within fluid conveyance systems, are extensively employed across aerospace, energy, chemical, power generation, and water supply sectors due to their reliable sealing performance and favourable regulating

characteristics.<sup>[1-3]</sup> Their core function involves altering the flow passage area through the vertical movement of the valve plug, thereby enabling pipeline isolation and flow throttling. During actual operation, the complex internal flow passage structure significantly modifies the fluid's motion state, leading to abrupt changes in local pressure and velocity.<sup>[4]</sup> Excessive internal pressure gradients readily induce localised low-pressure vortex zones downstream of the valve orifice. This not only increases localised fluid resistance losses and reduces system efficiency but may also trigger cavitation and erosion phenomena, generating vibrations and noise. Consequently, valve service life is shortened, potentially jeopardising the safe and stable operation of the entire pipeline system.<sup>[5,6]</sup>

In recent years, with the rapid advancement of computational fluid dynamics (CFD) technology, numerical simulation has become the mainstream approach for investigating complex flow fields within valves.<sup>[7]</sup> Compared to traditional experimental methods, CFD offers advantages such as lower cost, shorter turnaround times, and the ability to obtain comprehensive flow field information, enabling precise characterisation of key parameters like pressure and velocity distribution within valves. Currently, numerous scholars have employed this methodology for in-depth investigations, primarily focusing on the following areas: Firstly, flow field analysis for specific opening degrees and operating conditions. For instance, Zhu Fengxia<sup>[8]</sup> and colleagues obtained velocity and pressure distributions for globe valves at 80% and 100% opening; Wang Qiantang<sup>[5]</sup> and others demonstrated the quantitative impact of parameter variations on cavitation severity through their investigation of globe valve cavitation characteristics. Thirdly, combining structural improvements with mechanism exploration, such as Song Zhiwei<sup>[9]</sup> conducting multi-opening simulations on a DN50 globe valve, optimizing the valve plug structure and analyzing its flow field characteristics and external performance.

However, a review of existing literature reveals that most studies either focus on flow mechanisms under specific operating conditions (e.g., single opening degree or velocity)<sup>[10]</sup>, or examine the quantitative impact of parameters on particular phenomena (e.g., cavitation)<sup>[6]</sup>, or conduct structural optimization and flow field analysis for specific valve models (e.g., small valves).<sup>[11]</sup> For large-bore standard globe valves widely used in industry (e.g., nominal bore 125 mm models), comparative analysis of internal pressure distribution under multi-velocity and multi-opening combinations remains insufficient, particularly systematic investigations revealing pressure gradient patterns, differential pressure variations,

and cavitation risk evolution. To address this research gap, this paper employs a 125mm nominal diameter industrial globe valve as its subject. A refined three-dimensional model and computational mesh were established, with numerical simulations conducted using the k- $\Omega$  turbulence model. The study systematically configured four typical operating conditions: inlet velocities of 10 m/s and 15 m/s, combined with valve openings of half-open and fully open. Objectives include: - Comparing pressure distribution contour characteristics across the valve body's inner wall, inlet/outlet, and multiple perspectives under varying conditions; Quantitatively revealing key parameters such as maximum pressure differential and low-pressure zone extent as functions of valve opening and flow velocity; - Assessing cavitation risk and system efficiency impacts under different operating conditions.

Through this research, the paper aims to provide direct data support and theoretical basis for: structural optimization of industrial globe valves (e.g., improving plug profile to reduce pressure loss); safe operating condition selection (avoiding prolonged operation in cavitation-prone ranges); and enhancing system operational efficiency.

## 2. COMPUTATIONAL MODEL AND METHODOLOGY

### 2.1 Globe Valve Parameters

The primary dimensional parameters of the globe valve are presented in Table 1.

**Table 1: Key Parameters.**

Key Parameters	Parameter Value	Unit
Nominal Diameter DN	125	mm
Total valve body length L	400	mm
Total height of valve body H	460	mm
Flange Outer Diameter D	245	mm
Screw hole centre distance D1	210	mm
Flange water line outer diameter D2	185	mm
Flange thickness b	22	mm

### 2.2 Calculation of the model

Using SolidWorks software, the model of the globe valve established in this paper is shown in Fig. 1.

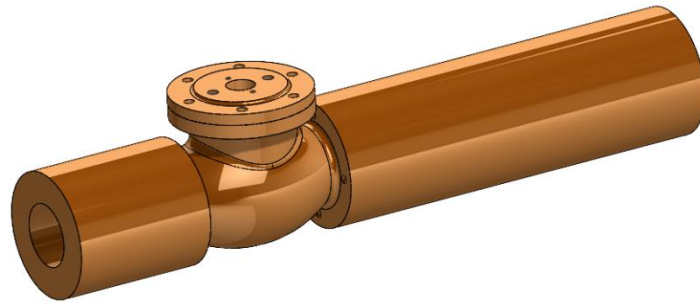


**Fig. 1.**

The cross-section of the globe valve is shown in Fig. 2. As depicted in Figure, the primary components subjected to pressure and wear are the pipe wall and the valve core.

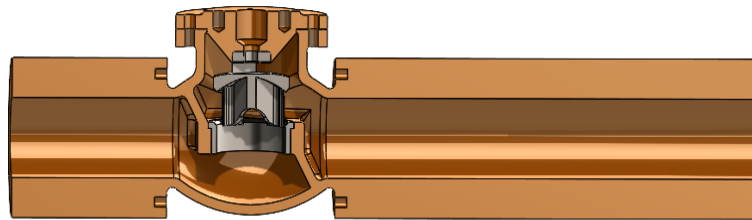


**Fig. 2: Cross-section of globe valve.**

### 2.3 Computational Mesh

The globe valve was meshed using ICEM software, yielding a total of 1,079,628 mesh elements overall. Under full operating conditions, the total number of mesh elements was 566,263. The inlet mesh of the globe valve is shown in Fig. 3

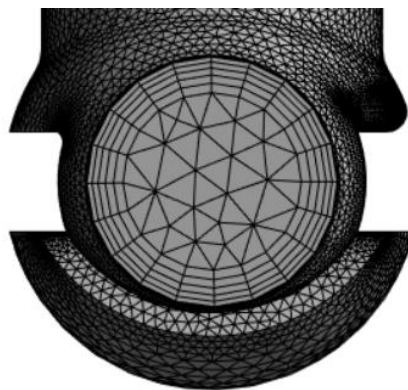


**Fig. 3: Inlet Mesh of the Globe Valve.**

The localised valve mesh is depicted in Fig. 4, whilst the overall valve mesh is shown in Fig. 5.

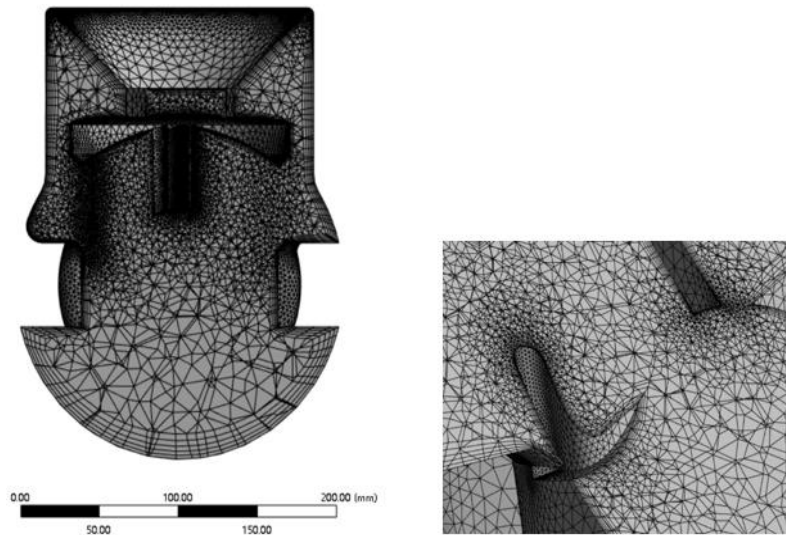


**Fig. 4: Local mesh for globe valve.**

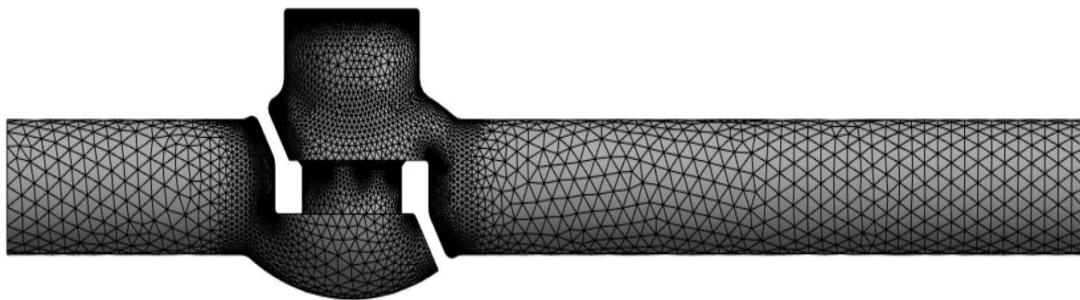


**Fig. 5: Computational Domain Full Mesh.**

## 2.4 Numerical Simulation Design

In model selection, the  $k - \Omega$  turbulence model was chosen for numerical simulation. During simulation, the left end of the globe valve was designated as the inlet, the right end as the outlet, and the inner wall as a wall surface. The computational scheme primarily defined four operating conditions: half-open and fully-open conditions with an inlet velocity of 10 m/s, and half-open and fully-open conditions with an inlet velocity of 15 m/s.

## 3. RESULTS ANALYSIS

Two valve opening conditions were selected for simulation: half-open and fully open. Each condition was subjected to two inlet velocities (10 m/s and 15 m/s), yielding four operational scenarios. Comparative analysis was conducted using cross-sectional views of both the pipeline and the globe valve.

### 3.1 Internal Pressure Distribution

Analysis of the internal wall pressure diagrams for the half-open and fully open conditions at an inlet flow velocity of 10 m/s is presented. The internal wall pressure diagrams are shown in Fig. 6.

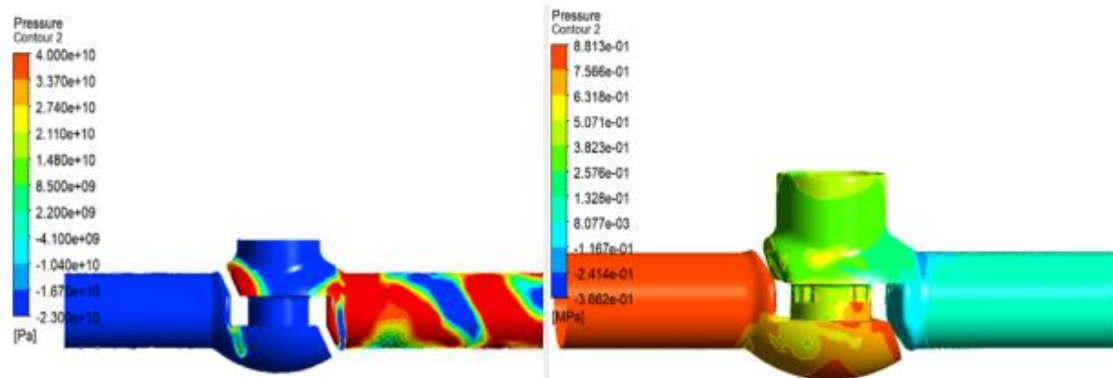


**Fig. 6: Internal wall Pressure Distribution at 10 m/s; Half-Open (Left) vs. Fully Open (Right).**

During the half-open state, the highest pressure within the concentrated high-pressure zone near the valve outlet reaches approximately 337 kPa. This significantly exceeds the upstream inlet gas pressure (set as a fixed value), with a discernible pressure differential between the two. As this region exhibits a pronounced red-to-blue color gradient indicative of high pressure gradients, it is evident that areas of higher local flow velocity correspond to lower pressure (consistent with Bernoulli's equation). Simultaneously, a low-pressure zone is observed downstream near the wall surface, where the pressure value reaches only approximately 22 kPa. This may give rise to low-pressure vortex regions, posing a risk of cavitation.

At fully open conditions, the pressure distribution becomes more uniform, with the maximum pressure decreasing to 85 kPa (a reduction of approximately 75% compared to half-open). This demonstrates that increasing valve opening reduces localised resistance. The pressure gradient diminishes (with broader color transition zones and smoother variations), and the downstream pressure distribution approaches a more reasonable range (approximately 41 kPa to 85 kPa). The anomalous low-pressure zone observed at full opening disappears, and the pressure values in the low-pressure zone converge towards a reasonable level (without extremely low pressure values). Consequently, the hydraulic performance at full opening is determined to be relatively stable.

At the half-open condition, the pressure differential across the valve opening is  $\Delta P = 337 \text{ kPa} - 22 \text{ kPa} = 315 \text{ kPa}$ , consistent with the throttling characteristics of globe valves, where pressure loss is proportional to the square of flow velocity. At the fully open condition, pressure loss reduces to 85 kPa to 41 kPa, i.e.,  $\Delta P = 44 \text{ kPa}$ . This demonstrates that valve opening affects system pressure loss, thereby influencing system efficiency.

Simultaneously, the inlet and outlet pressure diagrams for both operating conditions were analysed. These diagrams are illustrated at (Fig. 7, Fig. 8). and. Comparing the diagrams for both conditions reveals that the maximum inlet pressure at full opening drops to 2.74 MPa (approximately 32% lower than at half opening), indicating that increasing valve opening effectively reduces local resistance. The outlet pressure established at 0.662 MPa, with minimal downstream pressure fluctuations and a differential pressure of merely 0.218 MPa, verifying that increased valve opening enhances system efficiency.

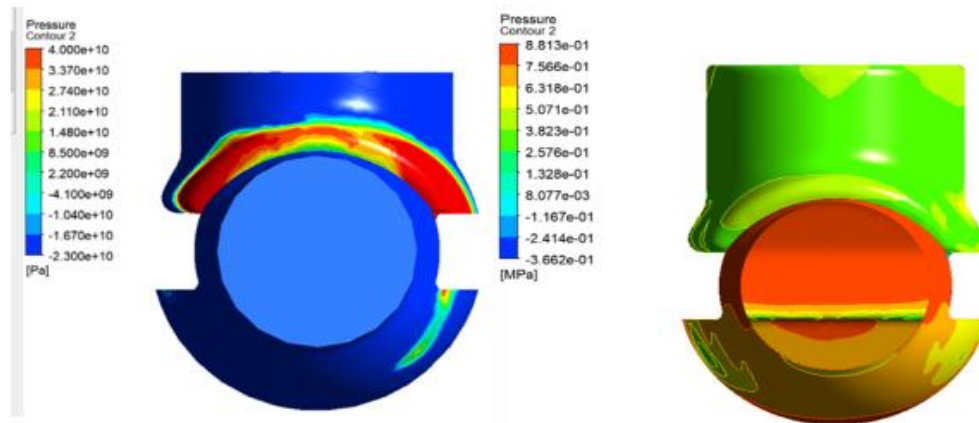


**Fig. 7: Pressure Distribution on the Inner Wall at the Inlet at 10 m/s; Half-Open (Left) vs. Fully Open (Right).**

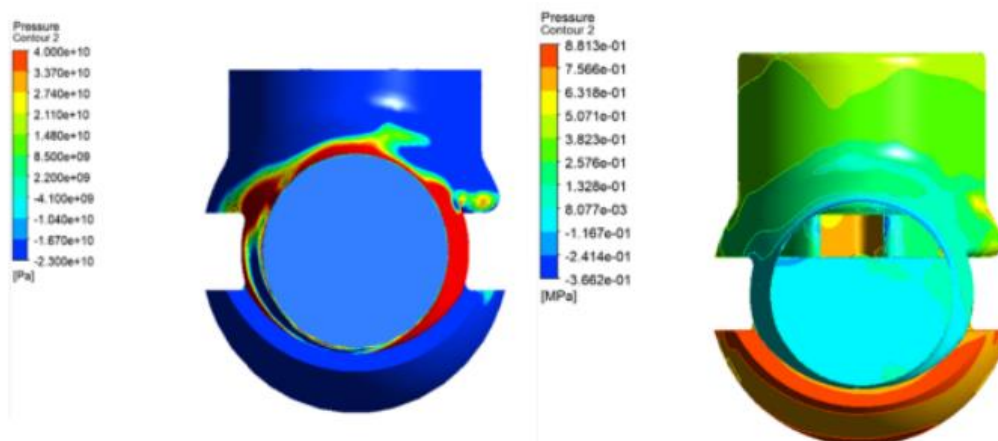


**Fig. 8: Pressure Distribution on the Inner Wall at the Outlet at 10 m/s; Half-Open (Left) vs. Fully Open (Right).**

vs. Fully Open (Right).

Observing the pressure distribution diagrams from different angles, as shown in Fig. 9 and Fig. 10.

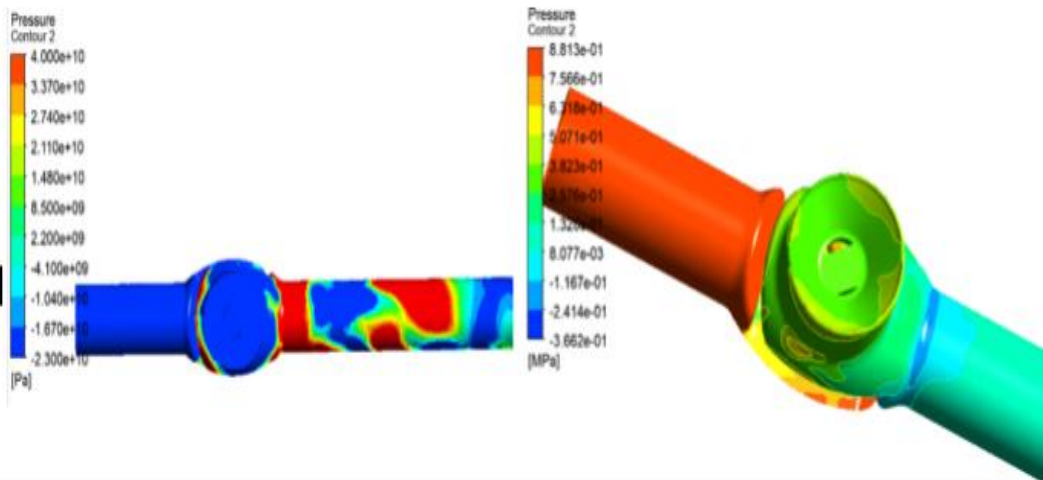


**Fig. 9: Pressure distribution on the upper inner wall at 10 m/s flow velocity: Half-Open (Left) vs. Fully Open (Right).**

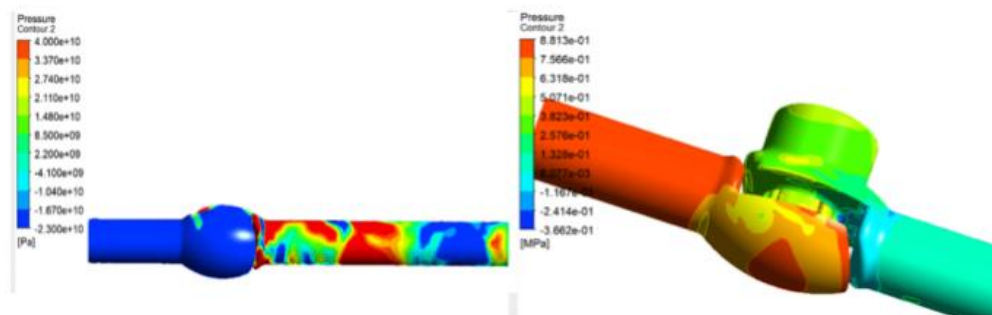


**Fig. 10: Pressure distribution on the lower inner wall at 10 m/s flow velocity: Half-Open (Left) vs. Fully Open (Right).**

To ensure the conclusions are as accurate as possible, the internal wall pressure diagrams for both the half-open and fully open conditions were reanalyzed at an inlet flow velocity of 15 m/s, as shown in Fig. 11, Fig. 12, Fig. 13, and Fig. 14.

Under the half-open condition, the maximum pressure difference reached 5.1 MPa, with rapid color transitions and steep gradients. In contrast, the fully open condition exhibited a maximum pressure difference of 2.8 MPa, characterized by uniform color transitions and gentle gradients. High-pressure zones were distributed at the upstream connection point of

the valve and downstream of the fully open valve core. When fluid flows through the valve, localized velocity surges cause sudden pressure drops (Bernoulli's equation). Furthermore, observation of the upstream high-pressure zone indicates good stability of the system inlet pressure. Low-pressure zones are distributed at the downstream far end and the outer side of the bend. The distribution of these low-pressure zones shows that after energy release in the high-pressure zone, downstream velocity decreases and pressure recovers.

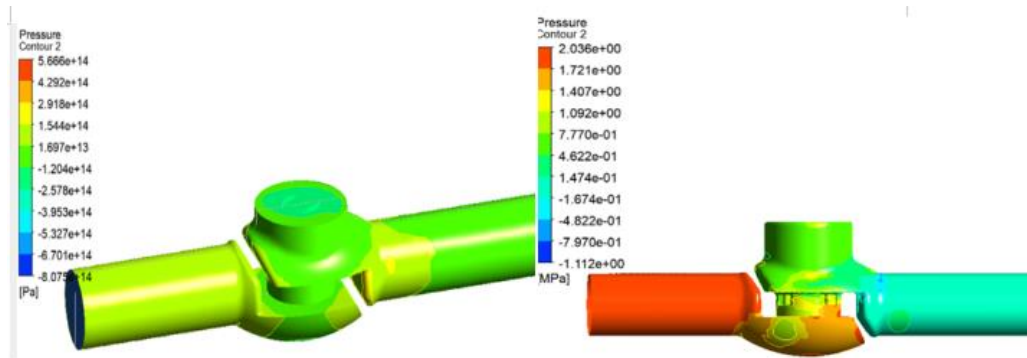


**Fig. 11: Pressure distribution on the inner wall at 15 m/s flow velocity Half-Open (Left) vs. Fully Open (Right).**

Observing the schematic diagram of the inner wall pressure from the inlet, outlet, and other perspectives, it is also evident that under identical flow rates, the fully operational condition exhibits a relatively smoother flow velocity change compared to the partially operational condition. At the inlet, the higher flow velocity results in greater pressure. Near the valve core, the flow velocity undergoes significant reduction, slowing down considerably. By the outlet, due to the multi-stage deceleration structure, the inner wall pressure at the outlet is already relatively low, resulting in a more moderate impact.

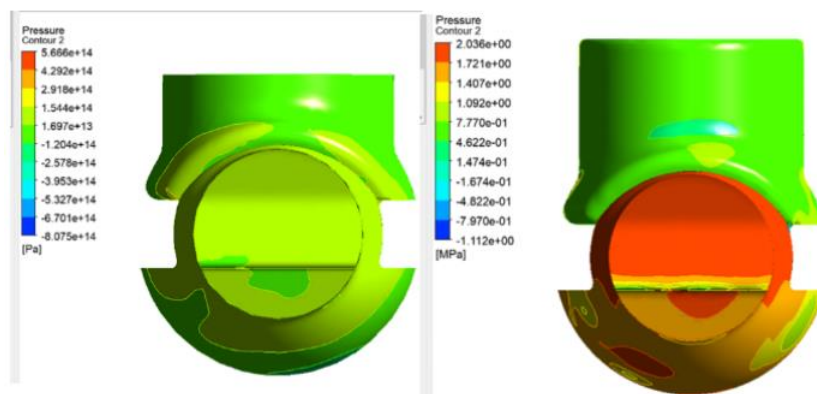


**Fig. 12: Pressure Distribution on the Inner Wall at the Inlet at 15 m/s; Half-Open (Left) vs. Fully Open (Right).**

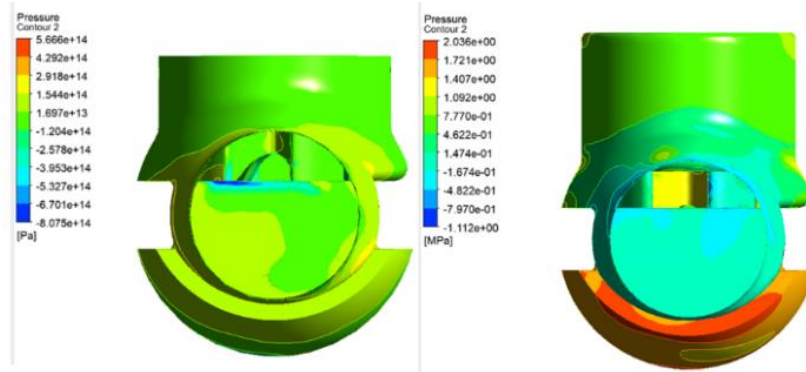


**Fig. 13: Pressure Distribution on the Inner Wall at the Outlet at 15 m/s; Half-Open (Left) vs. Fully Open (Right).**

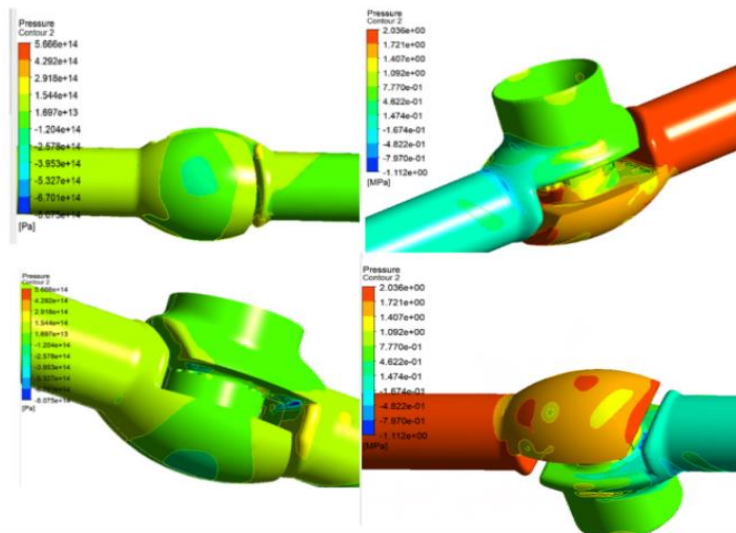


**Fig. 14: Pressure Distribution on the Inner Wall at Full and Half-Open Conditions for a 15 m/s Flow Velocity from Different Perspectives.**

Based on the aforementioned data, it can be concluded that high pressure is concentrated at the pipe fitting transition points and downstream of the valve opening, while low-pressure zones are distributed at the distal end of bends and in the downstream vortex region. The smaller the valve opening, the greater the pressure differential, and the higher the risk of cavitation and vibration.

#### 4. CONCLUSIONS

Under fully open conditions, the pressure distribution within the valve is more uniform with a gentler pressure gradient. At a flow velocity of 10 m/s, the maximum pressure differential decreases significantly from 337 kPa under half-open conditions to 85 kPa under fully open conditions; at 15 m/s, the maximum pressure differential reduces from 5.1 MPa to 2.8 MPa.

In the half-open state, a pronounced throttling effect occurs at the valve orifice, forming distinct high-pressure zones and high-velocity jets. These jets induce severe flow separation downstream of the valve body and at wall bends, creating extensive low-pressure vortex regions.

### ACKNOWLEDGMENT

The research was financially supported by the national college student science and technology innovation project (No.202411488043) and Science and Technology Project of Quzhou (No.2025K278).

### REFERENCE

1. Yan N H, Tang Y, Quan C R, et al. The exploring technique and the status quo of the stop valve of the high pressure air of the marine [J]. *Ship Engineering*, 2009; 31(S1): 67-70,97.
2. Lu L Q, Li Y P. The Internal Pneumatic Globe Valve Suitable for Liquid Hydrogen Transportation Pipelines [J]. *Valve*, 2024; 12: 1490-1493.
3. Zhang A. Research on flow field characteristics and structural optimization of nuclear power globe valve [D]. Dalian University of Technology, 2025.
4. Shang Z H. The Effect of Valve Spool Structure on the Performance of the Throttle Cut-off Valve [D]. Zhejiang Sci-Tech University, 2013.
5. Wang Q T, Wang J Y, Zhang K P, et al. Analysis of Cavitation Characteristics of Stop Throttle Valve [J]. *Chinese Journal of Vacuum Science and Technology*, 2023; 43(8): 715-723.
6. Gao Z X. Study on the Cavitation Mechanism and Control Methods of the Throttling Section in Valves [D]. Zhejiang University, 2020.
7. Yan C, Yu J, Xu J L, et al. On the achievements and prospects for the methods of computational fluid dynamics. [J]. *Advances in Mechanics*, 2011; 41(5): 562-589.
8. Zhu F X. Study on Flow Field Characteristics of Electric Globe Valves Based on CFD Technology [J]. *Mechanical Engineering & Automation*, 2021; 2: 55-56,58.
9. Song Z W. Numerical simulation of internal flow and test research of cut-off valve [D]. Zhejiang Sci-Tech University, 2012.
10. Chen Y, Wei W P, Zhang L X, et al. Flow Distribution Analysis in Break Valve Based on Fluent [J]. *Coal Mine Machinery*, 2013; 34(10): 90-91.
11. Jin K D, Yu W, Shang Y L, et al. Finite Element Analysis and Optimal Design of Liquid Helium Liquid Hydrogen Globe Valve [J]. *Valve*, 2024; 5: 544-547.